

Low-Temperature DC Carrier Transport in $(\text{Co}_{0.45}\text{Fe}_{0.45}\text{Zr}_{0.10})_x(\text{Al}_2\text{O}_3)_{1-x}$ Nanocomposites Sputtered in Mixed Argon–Oxygen Atmosphere

I.A. SVITO^a, A.K. FEDOTOV^a, A. SAAD^b, T.N. KOLTUNOWICZ^{a,*}, P. ZUKOWSKI^c
AND P. BURY^d

^aBelarusian State University, Independence av. 4, 220030 Minsk, Belarus

^bAl Balqa Applied University, Physics Department, P.O. Box 4545, Amman 11953, Jordan

^cDepartment of Electrical Devices and High Voltages Technologies, Lublin University of Technology
Nadbystrzycka 38a, 20-618 Lublin, Poland

^d University of Žilina, Univerzitna 1, 010 26 Žilina, Slovakia

This paper studies the temperature dependences ($2 < T < 300$ K) of the DC conductivity $\sigma(T)$ for the $(\text{Co}_{0.45}\text{Fe}_{0.45}\text{Zr}_{0.10})_x(\text{Al}_2\text{O}_3)_{1-x}$ nanocomposites ($30 < x < 65$ at.%) sputtered in Ar + O₂ atmosphere. It is shown that at temperatures lower than 100–150 K dependences of DC conductance on temperature for all the studied samples are due to the Shklovski–Efros variable range hopping mechanism. It was also observed that $\sigma(x, T)$ dependences can be attributed to the formation of FeCo-based oxide “shells” around metallic alloy nanoparticles due to incorporation of oxygen in the vacuum chamber during the deposition procedure.

DOI: [10.12693/APhysPolA.125.1351](https://doi.org/10.12693/APhysPolA.125.1351)

PACS: 73.22.–f, 72.20.Ee, 64.60.ah

1. Introduction

Composite materials containing metallic ferromagnetic nanoparticles in dielectric matrixes have potential applications as materials for magnetoelectronics [1]. One of the reasons for this interest lies in the tendency to miniaturization of the electromagnetic devices and improvement of their performance at higher frequencies [2]. Moreover, up to now, there is no complete understanding regarding the carrier transport mechanisms in the metal-dielectric composites, when dimensions of the metallic particles are approaching the nanometer scale.

Nanocomposites containing FeCo-based nanoparticles in dielectric matrix are one of the promising objects among film composites applicable in magnetoelectronic devices working in AC/DC modes. The characteristics of their carrier transport should be strongly dependent on the composition of the material, and in particular, on the position of the percolation threshold x_c and also some geometrical parameters of the metallic and dielectric phases (dimensions, shape, topology of distribution and scattering by various sizes of the nanoparticles) [2–5].

The goal of this work is to study the influence of metal-to-dielectric phase ratio x (its position relative to the percolation threshold) and also partial pressure of oxygen in Ar + O₂ gas mixture in the vacuum chamber on the carrier transport mechanisms estimated from the temperature dependences of the DC conductivity in the films, consisting of crystalline CoFeZr-alloy nanoparticles embedded into amorphous aluminum oxide matrix.

2. Experimental

The $(\text{Co}_{0.45}\text{Fe}_{0.45}\text{Zr}_{0.10})_x(\text{Al}_2\text{O}_3)_{1-x}$ nanocomposites thin film with $0.31 < x < 0.64$ and thicknesses d of 3–5 μm were fabricated by DC ion sputtering of the compound target onto the motionless glass ceramic substrate. Sputtered targets were composed of Fe_{0.45}Co_{0.45}Zr_{0.1} alloy plates, covered with strips of amorphous alumina. The deposition was carried out in a vacuum chamber evacuated down to 1×10^{-4} Pa and then filled with mixture of pure argon and oxygen. The common pressure in the chamber was 2.6×10^{-4} Pa, where the argon and oxygen partial pressures were about 6.7×10^{-2} Pa and 4.2×10^{-3} Pa, respectively [6].

The structure and composition of the as-deposited films were studied using the LEO 1455VP scanning electron microscope (SEM) with a special energy dispersive X-ray (EDX) microprobe, X-ray Empyrean PAN analytical diffractometer (XRD), Mössbauer spectrometer MS2000 with ⁵⁷Fe/Rh source, the Rutherford backscattering spectrometry (RBS) (see [4, 6]). Microstructural studies with electron diffraction (SAED) were also made using Philips EM400T transmission electron microscope (TEM), operated at 120 kV, and Philips CM200 operated at 200 kV for high resolution analysis (HRTEM). EDX SEM and RBS measurements were performed for checking the samples' stoichiometry with accuracy of $\approx 1\%$, confirming x and Fe/Co/Zr relation to be close to the nominal [6]. XANES and EXAFS measurements were performed for the beam line ID26 of the European Synchrotron Radiation Facility using high energy resolution fluorescence detection (HERFD) [6, 7]. Thicknesses of the films were measured on SEM with accuracy of $\approx 2\text{--}3\%$ on cleavages of the samples studied.

corresponding author; e-mail: t.koltunowicz@pollub.pl

The rectangular samples with dimensions of 10 mm \times 2 mm \times d μ m for electric measurements were cut from nanocomposite. Four indium contacts were deposited by ultrasound soldering on the top of every sample to make four-probe DC conductivity σ and I - V characteristics measurements. To make temperature dependences of conductivity $\sigma(T)$ between 2 and 300 K the sample inserted into a closed-cycle Cryogen-Free Cryostat System CFCS (Cryogenic Ltd., London, GB). The PC based control system with Lakeshore Temperature Controller (Model 331) allowed either to change the temperature with a rate of 0.1–1 K/min (both in cooling and heating regimes) or to stabilize it with accuracy of 0.005 K during long time (not less than 1 h). The relative error of conductance measurements was less than 0.1%.

3. Results and discussion

The comparison of SEM, XRD, TEM, SAED, X-ray absorption near-edge structure (XANES), extended X-ray absorption fine structure (EXAFS), and Mössbauer data for the studied samples, presented in [3, 4, 6], has allowed to make the following conclusions concerning their phase structure. Granular films of $(\text{Co}_{0.45}\text{Fe}_{0.45}\text{Zr}_{0.10})_x(\text{Al}_2\text{O}_3)_{1-x}$ sputtered in atmosphere with added oxygen contained FeCo-based nanoparticles with “metallic core–oxide shell” structure. Formation of such a structure, composed of crystalline metallic bcc α -FeCo-based nanosized “cores” encapsulated in FeCo-based oxide “shells”, all embedded in the amorphous alumina matrix, was revealed with TEM and

HRTEM. EXAFS and XANES exhibited almost full oxidation of iron, but cobalt only was found to be partially oxidized. In strong correlation with the Mössbauer spectroscopy together with the results of electron- and X-ray diffraction they showed that for $x \leq 0.56$ the metallic “core” constituted bcc FeCo solid solution, possibly enriched with Co, while oxide “shell” mainly consisted of mixed Fe-rich oxide. Moreover, as was shown in [6], addition of oxygen to the chamber suppressed agglomeration and strong scattering by various sizes of the alloy nanoparticles and that was observed in the films deposited in pure Ar gas [8].

The dependence of conductivity σ on concentration x for the metallic fraction of $(\text{Fe}_{0.45}\text{Co}_{0.45}\text{Zr}_{0.10})$ alloy in the studied films is shown in Fig. 1a. As is seen, the measured $\sigma(x)$ curve does not display sigmoid-like shape as usually observed in many of metal–insulator nanocomposites. Moreover, the values of conductivity are approximately 3 orders of magnitude lower than was observed in the same nanocomposites deposited in pure Ar atmosphere in vacuum chamber [4]. This confirms the above mentioned formation of FeCo-based oxide “shells”. The $\sigma(x)$ behavior for the studied nanocomposites can be divided into 3 characteristic parts which are determined by the progress of the enhanced selective oxidation of the $(\text{Fe}_{0.45}\text{Co}_{0.45}\text{Zr}_{0.10})$ alloy nanoparticles with the concentration x increase during the deposition procedure as was proved in [6].

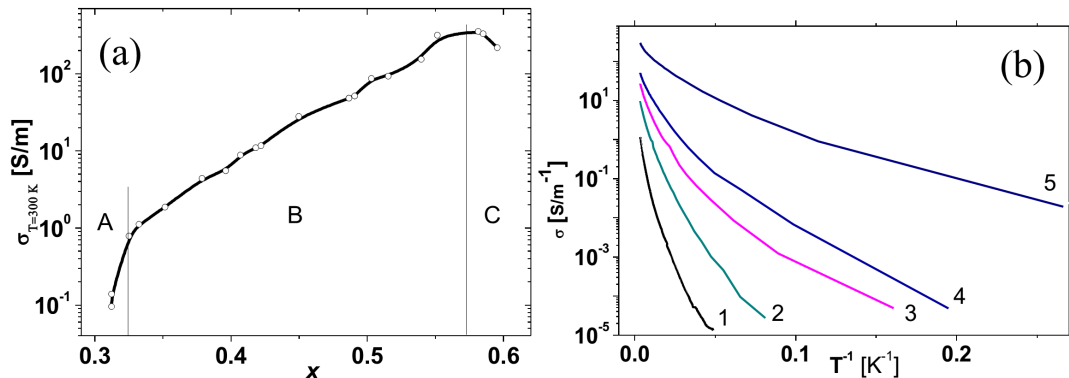


Fig. 1. Dependences of the DC conductivity ($T = 298$ K) on the metal-to-dielectric ratio x (a) and on temperature (b) (in the Arrhenius scale) for $x = 0.33$ (1), 0.41 (2), 0.45 (3), 0.50 (4), 0.62 (5).

Temperature dependences of DC conductivity are presented in Fig. 1b in the Arrhenius scales. The $\sigma(T)$ figures show that all the samples studied (belonging to all 3 regions A–C) display $(d\sigma/dT) > 0$, that is characteristic for thermally activated carrier transport on the insulating side of the insulator–metal transition (IMT). Moreover, the samples of region A have higher and sharper slopes in the low-temperature range (see curve 1 in Fig. 1b) compared to that of regions B and C i.e. the positive slopes $(d\sigma/dT)$ of $\sigma(T)$ curves in the Arrhenius scale for the samples of region B and especially of region C were

lower (curves 2–5). Let us note also that even beyond the $x_{\text{max}} \approx 0.57$ there was no observation of transition to metallic state with the power like $\sigma(T)$ dependences (as in the films deposited in the same sputtering conditions but in pure Ar atmosphere in the chamber, see [4, 8]). The above mentioned results indicated that the concentration x_{max} , where $\sigma(x)$ curves exhibit maximum, can be considered as the concentration when the oxidized FeCoZr nanoparticles become to contact to each other forming continuous and highly-conductive net in the region C of Fig. 1a.

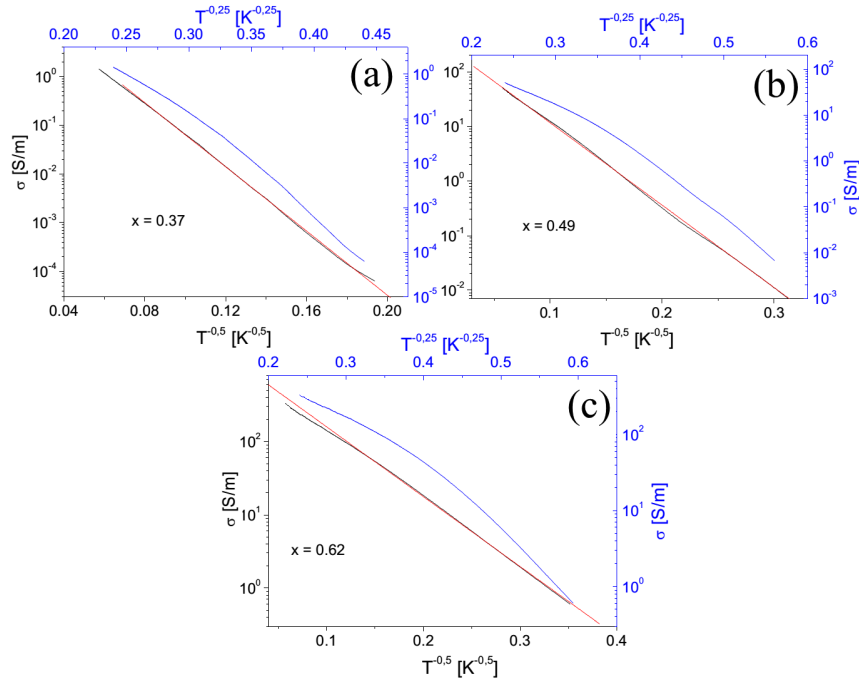


Fig. 2. Temperature dependences of the conductivity $\sigma(T)$ for the samples of $x = 0.315$ (a), 0.491 (b) and 0.615 (c) plotted in the Mott scale with the exponent $n = 0.5$ (lower curves 1 and 1') and $n = 0.25$ (upper curves 2 and 2') using relation (1). 1, 2 — experimental data, 1', 2' — linear approximations of $\ln \sigma - T^{-n}$.

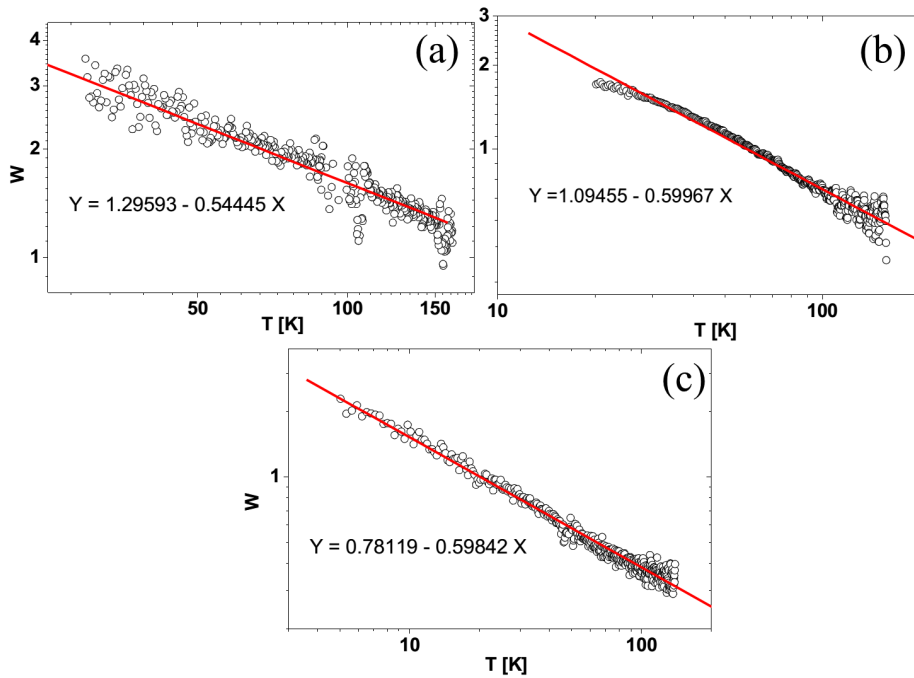


Fig. 3. Temperature dependences of $w(T)$ in a double logarithmic scale for the samples of $x = 0.315$ (a), 0.491 (b), and 0.615 (c). Circles are experimental points and solid lines are approximations by the relation (2).

Discussion of the obtained $\sigma(x, T)$ dependences for the studied samples, belonging to different regions A , B , and C in Fig. 1a, on carrier transport mechanisms is given as follows. The experimental curves in Fig. 2 were re-plotted in the Mott scale, and show that all the

samples exhibited exponential-like character of $\sigma(T)$ dependences with the change (reduction) of the activation energy as the temperature decreased. Such behavior indicated the variable range hopping (VRH) mechanism of conductance which follows the known Mott relation:

$$\sigma(T) = \sigma_0 \exp\left(- (T_0/T)^{-n}\right), \quad (1)$$

where σ_0 and T_0 are characteristic parameters of the VRH models and the exponent n in (1) equals 0.25 for Mott mechanism [9] and 0.50 for the Shklovski–Efros model [10]. In order to understand the nature of the VRH mechanism in our case and to specify the real value of the exponent n in (1), the Zabrodski method [11] was used. This method is based on the analysis of temperature dependences of the reduced activation energy

$$w = -\frac{1}{T} \frac{\partial \ln \sigma}{\partial (1/T)}. \quad (2)$$

In accordance with this approach, if the $\sigma(T)$ dependences are described by formulae (1) for VRH hopping mechanism, the exponent n can be extracted from the relation

$$\lg w = A - n \lg T, \quad (3)$$

which follows from (2).

Figure 3 presents the $w(T)$ dependences plotted after graphic procedure of differentiation and the following fitting by relation (3) $Y = A + nX$ (see insets in Fig. 3a–c), where $Y = \ln w$ and $X = \ln T$. Results of the presented experimental work have shown that, for the studied composites at temperatures lower than 120–150 K, the exponent n (i.e. slopes of linear approximations (3) in Fig. 3a–c) has changed between 0.54 and 0.60, that is close to the $n = 0.5$ for the Shklovski–Efros model, describing the VRH transport at the presence of the Coulomb gap in the energy distribution of the localized states density due to electron–electron interaction. This is also confirmed by better linearization of $\sigma(T)$ curves, shown in Fig. 2, using the Shklovski–Efros relationship with $n = 0.5$.

4. Resume

The presented work has shown that the temperature dependences of the DC conductivity $\sigma(T)$ of the $(\text{Co}_{0.45}\text{Fe}_{0.45}\text{Zr}_{0.10})_x(\text{Al}_2\text{O}_3)_{1-x}$ nanocomposites, deposited in mixed Ar+O₂ gas atmosphere, displayed the Shklovski–Efros VRH mechanism for the carrier transport which occurred at temperatures lower than 120–150 K. The observed $\sigma(x, T)$ dependences can be attributed to the formation of FeCo-based oxide “shells” around metallic alloy nanoparticles due to the addition of oxygen into the vacuum chamber during the deposition procedure.

Acknowledgments

The work was partially supported by the VISBY Program of the Swedish Institute and Belarusian State Sub-Programme “Crystalline and Molecular Structures” by contract 2.4.12 and a research project No. IP2012 026572 within the Iuventus Plus program of Polish Ministry of Science and Higher Education in the years of 2013–2015. Doctor T.N. Koltunowicz is a participant of the project: “Qualifications for the labour market — employer friendly university”, cofinanced by European Union from European Social Fund.

References

- [1] Y. Imry, in: *Nanostructures and Mesoscopic Systems*, Eds. W.P. Kirk, M.A. Reed, Academic, New York 1992.
- [2] G. Timp, *Nanotechnology*, Springer, New York 1999.
- [3] T.N. Koltunowicz, P. Zukowski, M. Milosavljević, A.M. Saad, J.V. Kasiuk, J.A. Fedotova, Yu.E. Kalinin, A.V. Sitnikov, A.K. Fedotov, *J. Alloys Comp.* **586**, S353 (2014).
- [4] J. Fedotova, in: *Advances in Nanoscale Magnetism*, Eds. B. Aktas, F. Mikailov, Springer Proceedings in Physics, Berlin 2008, p. 122, 231.
- [5] G. Grimmet, *Percolation*, 2nd ed., Springer-Verlag, Berlin 1999.
- [6] J. Fedotova, J. Przewoznik, C. Kapusta, M. Milosavljević, J.V. Kasiuk, J. Zukowski, M. Sikora, A.A. Maximenko, D. Szepletowska, K.P. Homewood, *J. Phys. D* **44**, 495001 (2011).
- [7] P. Glatzel, M. Sikora, S.G. Eeckhout, O.V. Safonova, G. Smolentsev, G. Pirngruber, van J.A. Bokhoven, J.D. Grunewaldt, M. Tromp, in: *Conf. Proc. 9th Int. Conf. on Synchrotron Radiation Instrumentation, Daegu (Korea)*, 2006, Vol. 879, AIP, New York 2007, p. 1731.
- [8] T.N. Koltunowicz, P. Zhukowski, V.V. Fedotova, A.M. Saad, A.V. Larkin, A.K. Fedotov, *Acta Phys. Pol. A* **120**, 35 (2011).
- [9] N.F. Mott, E.A. Davis, *Electron Process in Non-Crystalline Materials*, Clarendon Press, Oxford 1979.
- [10] A.L. Efros, B.I. Shklovski, *Phys. Status Solidi B* **76**, 475 (1976).
- [11] A.G. Zabrodski, *Sov. Solid State Phys.* **11**, 595 (1977).